

Label Propagation for Graph Label Noise

Yao Cheng
East China Normal University
Shanghai, China
yaocheng_623@stu.ecnu.edu.cn

Caihua Shan
Microsoft Research Asia
Shanghai, China

Yifei Shen
Microsoft Research Asia
Shanghai, China

Xiang Li
East China Normal University
Shanghai, China

Siqiang Luo
Nanyang Technological University
Singapore

Dongsheng Li
Microsoft Research Asia
Shanghai, China

ABSTRACT

Label noise is a common challenge in large datasets, as it can significantly degrade the generalization ability of deep neural networks. Most existing studies focus on noisy labels in computer vision; however, graph models encompass both node features and graph topology as input, and become more susceptible to label noise through message-passing mechanisms. Recently, only a few works have been proposed to tackle the label noise on graphs. One major limitation is that they assume the graph is homophilous and the labels are smoothly distributed. Nevertheless, real-world graphs may contain varying degrees of heterophily or even be heterophily-dominated, leading to the inadequacy of current methods.

In this paper, we study graph label noise in the context of arbitrary heterophily, with the aim of rectifying noisy labels and assigning labels to previously unlabeled nodes. We begin by conducting two empirical analyses to explore the impact of graph homophily on graph label noise. Following observations, we propose a simple yet efficient algorithm, denoted as LP4GLN. Specifically, LP4GLN is an iterative algorithm with three steps: (1) reconstruct the graph to recover the homophily property, (2) utilize label propagation to rectify the noisy labels, (3) select high-confidence labels to retain for the next iteration. By iterating these steps, we obtain a set of “correct” labels, ultimately achieving high accuracy in the node classification task. The theoretical analysis is also provided to demonstrate its remarkable denoising effect. Finally, we conduct experiments on 10 benchmark datasets under varying graph heterophily levels and noise types, comparing the performance of LP4GLN with 7 typical baselines. Our results illustrate the superior performance of the proposed LP4GLN.

ACM Reference Format:

Yao Cheng, Caihua Shan, Yifei Shen, Xiang Li, Siqiang Luo, and Dongsheng Li. 2018. Label Propagation for Graph Label Noise. In *Proceedings of Make sure to enter the correct conference title from your rights confirmation email (Conference acronym 'XX)*. ACM, New York, NY, USA, 15 pages. <https://doi.org/XXXXXXXXXXXX.XXXXXXXXXX>

Permission to make digital or hard copies of all or part of this work for personal or classroom use is granted without fee provided that copies are not made or distributed for profit or commercial advantage and that copies bear this notice and the full citation on the first page. Copyrights for components of this work owned by others than ACM must be honored. Abstracting with credit is permitted. To copy otherwise, or republish, to post on servers or to redistribute to lists, requires prior specific permission and/or a fee. Request permissions from [permissions@acm.org](https://permissions.acm.org).
Conference acronym 'XX, June 03–05, 2018, Woodstock, NY

© 2018 Association for Computing Machinery.
ACM ISBN 978-1-4503-XXXX-X/18/06...\$15.00
<https://doi.org/XXXXXXXXXXXX.XXXXXXXXXX>

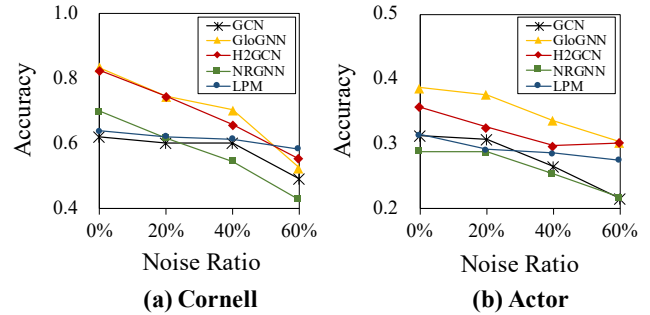


Figure 1: The classification accuracy with flip label noise ranging from 0% to 60% on Cornell and Actor datasets.

1 INTRODUCTION

Graphs are ubiquitous in the real world, such as social networks [13], biomolecular structures [35] and knowledge graphs [8]. In graphs, nodes and edges represent entities and their relationships respectively. To enrich the information of graphs, each node is usually associated with a descriptive label. For example, each user in Facebook has interest as its label. Recently, to learn from graphs, graph neural networks (GNNs) have achieved significant success, which can seamlessly integrate node features with graph structure to learn node representations. GNNs generally adopt the message passing strategy to aggregate information from nodes’ neighbors and then update node representations. After that, the learned representations are fed into various downstream tasks, such as node classification.

Despite their great performance, GNNs still encounter challenges from label noise, which is a pervasive issue in real-world datasets. For example, non-expert sources like Amazon’s Mechanical Turk and web pages can be used to collect labels, which could unintentionally lead to unreliable labels and noise. It is well known that deep neural networks are very sensitive to noise, thereby degrading their generalization ability [30]. To address the problem, there have been a majority of neural network models [9, 17, 18, 29] proposed in the field of computer vision (CV) to tackle label noise in images. Unfortunately, we cannot directly apply these approaches to graph-structured data as graphs are non-Euclidean data types. Therefore, exploring the issue of graph label noise is highly necessary.

Recently, very few works have been proposed to deal with graph label noise [3, 27]. These models still attenuate graph label noise based on an explicit *homophily* assumption that linked nodes in a graph are more likely to be with the same label. However, homophily is not a universal principle in the real world. In fact,

graph datasets often exhibit varying degrees of homophily, and may even be heterophily-dominated. Methods based on the homophily assumption evidently cannot handle these heterophilous graphs. As shown in Figure 1, we compare the performance of GCN, H₂GCN [32] and GloGNN [15], which are specially designed for homophilous and heterophilous graphs, against two state-of-the-art methods for graph label noise, LPM [27] and NRGNN [3], on the heterophilous benchmark dataset *Cornell* and *Actor* with flip noise¹ ranging from 0% to 60%. The results indicate that on heterophilous graphs, current methods for label noise (LPM and NRGNN), are still underperformed by GNN models designed for graph heterophily (H₂GCN and GloGNN). The problem of graph label noise deserves further investigation.

In this paper, we study graph label noise in the context of arbitrary heterophily, with the aim of rectifying noisy labels and assigning labels to previously unlabeled nodes. We first explore the impact of graph homophily on graph label noise by conducting a series of experiments on benchmark heterophilous datasets. Specifically, we manipulate graph homophily by graph reconstruction to see if existing methods could improve their classification performance against label noise. The observations demonstrate that a high graph homophily rate can indeed mitigate graph label noise. In addition, we find that label propagation (LP) [34] based methods achieve great performance as graph homophily increases.

These inspirations led us to propose a simple yet effective algorithm, LP4GLN. We further refine this basic solution in several aspects. In terms of effectiveness, we implement a multi-round selection process as opposed to correcting noisy labels all at once. Specifically, we select high-confidence noisy labels to augment the correct label set, and then repeat the algorithm, achieving higher accuracy. With respect to efficiency, we reduce the time complexity to linear time by unifying the computation of graph construction and label propagation. Ultimately, we provide a theoretical proof of LP4GLN, illustrating its impressive denoising effect in addressing graph label noise.

To summarize, our main contributions are:

- **Empirical Analysis:** We first investigate the influence of graph homophily on label noise through the manipulation of homophily levels and noise ratios within real-world datasets. Moreover, we incorporate three common homophilous graph reconstruction modules into existing approaches, to evaluate the performance improvement of these approaches in heterophilous graphs.
- **Algorithm Design and Theoretical Proof:** Based on empirical observations, we propose a simple yet effective algorithm LP4GLN to deal with the issue of graph label noise. Specifically, LP4GLN is an iterative algorithm with three steps: (1) reconstruct the graph to recover the homophily property, (2) utilize label propagation to correct the noisy labels, (3) select high-confidence corrected labels and add them to the clean label set to retain for the next iteration. By repeating these steps, we obtain a set of “correct” labels to achieve accurate node classification. We also provide a theoretical analysis of the denoising effect of LP4GLN.
- **Extensive Experiments:** We conduct extensive experiments on two homophilous datasets and eight heterophilous datasets with varying noise types and ratios. Our proposed LP4GLN outperforms

baselines in the majority of cases, demonstrating the superior performance of LP4GLN. The ablation studies are also done to verify the necessity of each component of LP4GLN.

2 PRELIMINARIES

Problem Definition. We consider the semi-supervised node classification task in an undirected graph $\mathcal{G} = (\mathcal{V}, \mathcal{E})$ where $\mathcal{V} = \{v_i\}_{i=1}^n$ is a set of nodes and $\mathcal{E} \subseteq \mathcal{V} \times \mathcal{V}$ is a set of edges. Let the label set as \mathcal{Y} with c classes, and $\mathcal{V} = \mathcal{C} \cup \mathcal{N} \cup \mathcal{U}$, where \mathcal{C} is set of labeled nodes with clean labels Y_C , \mathcal{N} is a set of labeled nodes with noise labels Y_N and \mathcal{U} is set of unlabeled nodes. Let A be the adjacency matrix of \mathcal{G} such that $A_{ij} = 1$ if there exists an edge between nodes v_i and v_j ; 0, otherwise. For the initial node feature matrix, we denote it as X . Our goal is to design an effective algorithm to predict the class label for noisy and unlabeled nodes.

GNN and Label Propagation Basics. Most graph neural networks follow the message-passing mechanism, which consists of two main steps: aggregation and update. GNNs first aggregate information from neighboring nodes $\hat{h}_i^{(l)} = \text{AGGREGATE}(h_j^{(l-1)}, \forall v_j \in \mathcal{N}_i)$, and then update each node embeddings $h_i^{(l)} = \text{UPDATE}(h_i^{(l-1)}, \hat{h}_i^{(l)})$. After L aggregations, the final node embedding $H^{(L)}$ is obtained and then fed into a softmax layer to generate probability logits for label prediction. Different from GNNs, label propagation directly aggregates the labels from neighboring nodes through the formula $Y_i^{(l)} = (1 - \alpha) \cdot Y_i^{(l-1)} + \alpha \cdot \text{AGGREGATE}(Y_j^{(l-1)}, \forall v_j \in \mathcal{N}_i)$. It converges when labels do not change significantly between iterations. Depending on the various utilization of labels, the robustness of GNNs and LP to graph label noise is also different.

3 HOW DOES HOMOPHILY IMPACT GRAPH LABEL NOISE?

In this section, we investigate the potential of mitigating graph label noise by decreasing the graph heterophily rate. To do this, we first outline existing approaches for graph label noise. Next, we introduce three graph reconstruction modules to transform the original graphs into homophilous ones. Ultimately, we modify the graph structure in heterophilous datasets through two manipulations: (1) converting the heterophilous edges into homophilous ones based on the ground-truth labels and (2) reconstructing the homophilous graph. We then apply the existing approaches to the modified datasets and several critical observations are derived from these experiments.

3.1 Existing Approaches

Here we introduce two state-of-the-art methods for graph label noise, LPM [27] and NRGNN [3].

- **LPM** is proposed to tackle graph label noise by combining label propagation and meta-learning. It consists of three modules: a GNN for feature extraction, LP for pseudo-label generation and an aggregation network for merging labels. Initially, the similarity matrix $A'_{ij} = \frac{A_{ij}}{d(h_i, h_j) + \tau}$ is calculated based on the adjacency matrix A and the node embeddings h_i and h_j . These embeddings are learned by the GNN feature extraction. The function $d(\cdot, \cdot)$ represents a distance measure, and τ is an infinitesimal constant. Then LP is

¹Flip noise and uniform noise are explained in Section 6.1.

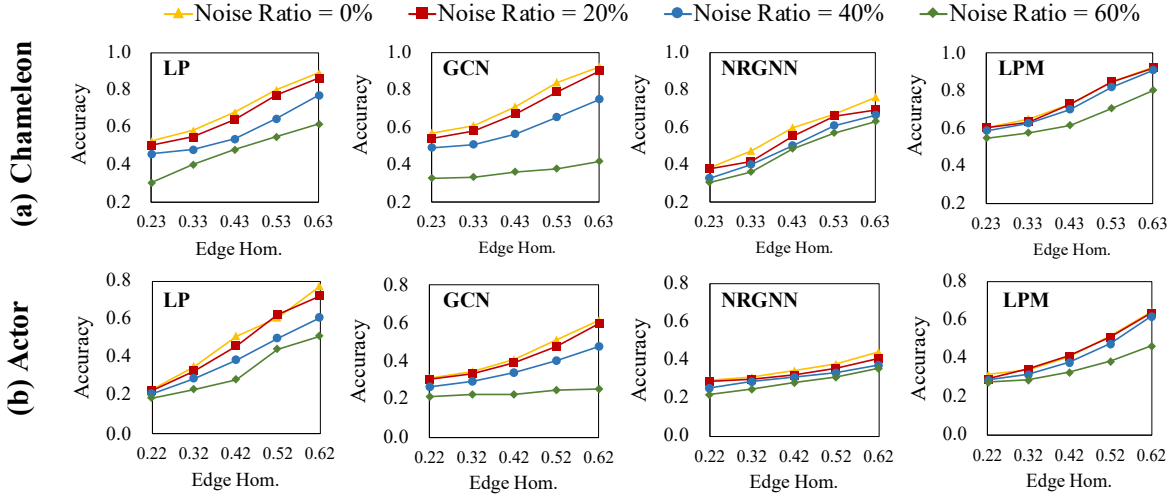


Figure 2: The impact of edge homophily on graph label noise across various methods (flip noise)

performed on A' to generate pseudo-labels. Lastly, the aggregation network is used to integrate the original labels and pseudo-labels, resulting in the final labels through meta-learning.

• **NRGNN** is also designed to deal with graph label noise and label sparsity, including three modules: an edge predictor, a pseudo-label predictor, and a GNN classifier. The edge predictor first generates extra edges to connect similar labeled and unlabeled nodes by the link prediction task. As a result, the newly generated adjacency matrix A' becomes denser. Then the pseudo-label predictor estimates pseudo-labels Y' for unlabeled nodes. The GNN classifier outputs the final predictions based on the updated A' and Y' .

Formally, the overall process of these two methods can be formulated into three steps:

$$\begin{aligned} A' &= f_{\text{reconstruct}}(A, X), \\ Y' &= f_{\text{pseudo-label}}(Y, A'), \\ Y_{\text{final}} &= f_{\text{predict}}(X, A', Y, Y'). \end{aligned} \quad (1)$$

Note that both LPM and NRGNN depend on the graph homophily assumption. Further, they mainly concentrate on pseudo-label generation, while overlooking the correction of noisy labels.

3.2 Graph Reconstruction with Homophily

While both LPM and NRGNN reconstruct the original graph, their methods have clear limitations. For LPM, it only adjusts the weights of raw edges in the graph, which cannot add new edges. Further, NRGNN employs link prediction as objective to predict new edges, which takes existing edges in the graph as positive samples. This restricts its wide applicability in graphs with heterophily. Therefore, we next introduce three common methods to convert heterophilous graphs into homophilous ones.

First, the goal is to directly construct a similarity matrix that serves as the homophilous graph. Specifically, we train a GNN $f(\cdot)$ to aggregate node features and topological structure, and obtain the hidden representation h_i for node v_i . We then simply calculate the distance between nodes by cosine similarity. The existence of

edge Z_{ij} between nodes v_i and v_j is decided by a fixed threshold ϵ :

$$Z_{ij} = 1 \text{ if } \text{distance}(h_i, h_j) < \epsilon; 0, \text{ otherwise} \quad (2)$$

This method can be considered as a direct extension to the one used by LPM. On the one hand, both methods compute the similarity between nodes based on node embeddings learned by GNN. On the other hand, our method can further add new edges into the graph, while LPM cannot.

The second option is to learn a new graph adjacency matrix. The representative method is GloGNN [15], which learns the hidden representation H for nodes and the new homophilous graph Z together. Specifically, in the l -th layer, it aims to obtain a coefficient matrix $Z^{(l)} \in \mathbb{R}^{n \times n}$ and node embeddings $H^{(l)} \in \mathbb{R}^{n \times d}$ satisfying $H^{(l)} \approx Z^{(l)} H^{(l)}$. Each element $Z_{ij}^{(l)}$ represents how well node v_j characterizes node v_i . The objective is formulated as:

$$\min_{Z^{(l)}, H^{(l)}} \|H^{(l)} - (1-\gamma)Z^{(l)}H^{(l)} - \gamma H^{(0)}\|_F^2 + \beta_1 \|Z^{(l)}\|_F^2 + \beta_2 \|Z^{(l)} - \sum_{k=1}^K \lambda_k \hat{A}^k\|_F^2, \quad (3)$$

where β_1 and β_2 are two hyper-parameters to control term importance. $H^{(0)}$ could be a simple transformation of initial node features X and adjacency matrix A (e.g., $\text{MLP}(\text{Concat}(X, A))$), and γ is to balance the importance of initial and current embeddings. \hat{A}^k denotes the k -hop sub-graph, and K is the pre-set maximum hop count. Equation 3 has a closed-form solution:

$$\begin{aligned} Z^{(l)*} &= \left[(1-\gamma)H^{(l)}(H^{(l)})^\top + \beta_2 \sum_{k=1}^K \lambda_k \hat{A}^k - \gamma(1-\gamma)H^{(0)}(H^{(l)})^\top \right] \\ &\cdot \left[(1-\gamma)^2 H^{(l)}(H^{(l)})^\top + (\beta_1 + \beta_2)I_n \right]^{-1}. \end{aligned} \quad (4)$$

Here, $Z^{(l)*}$ characterizes the connections between nodes. After L layers, we use $Z^{(L)*}$ to denote homophilous graph structure.

In the third option, $Z^{(L)*}$ can be further adjusted to be symmetric and non-negative. Formally, we add the following formula after the calculation of Equation 4, and still optimize the objective in

Equation 3:

$$\hat{Z}^{(L)} = \text{ReLU}\left(\frac{1}{2}(Z^{(L)*} + (Z^{(L)*})^T)\right). \quad (5)$$

3.3 Empirical Analysis

We next investigate the relationship between graph homophily and graph label noise using two types of empirical experiments. In the first experiment, we directly enhance the homophily level by converting heterophilous edges into homophilous ones based on the ground-truth labels, and then run existing methods to compare their performance. In the second experiment, we integrate the three homophilous graph reconstruction modules with existing approaches and evaluate them in heterophilous datasets.

3.3.1 Graph Homophily Mitigates Graph Label Noise. We modified the edge homophily level and label noise level on two real-world heterophilous datasets, *Chameleon* and *Actor*. In order to maintain the same sparsity of the dataset, we randomly replace a heterophilous edge in the original graph with a homophilous one. We conducted experiments on four methods, including two classical methods: LP and GCN; and two SOTA methods for graph label noise: NRGNN and LPM. Figure 2 shows the performance of all the methods under different levels of flip label noise. The results for uniform label noise are given in Figure 7 in Appendix D.1.

From the figures, we observe that: (1) For all the methods and noise rates, the classification accuracy consistently improves with the increase of graph homophily on both *Chameleon* and *Actor* datasets. Surprisingly, when graph homophily gets larger, even under a high noise rate (e.g., 0.6 for LP, NRGNN and LPM, 0.4 for GCN), these methods can still achieve better performance than their corresponding results in the original heterophilous graph without label noise. This indicates that graph homophily can effectively mitigate the negative impact of label noise. (2) When the noise rate is 0.6, GCN performs poorly, while LP can still achieve the best results among all the methods in some cases. This shows that although both GCN and LP apply the smoothing operation on node features and labels, respectively, GCN is adversely affected by the coupling of node features and learnable transformation matrix, which is also pointed out in [12]. This insight also demonstrates that LP excels at correcting noisy labels through label smoothing under various conditions of graph homophily. We will give theoretical proofs in Sec. 4.4 later. To sum up, all the results empirically show that graph homophily plays a significant role in denoising labels.

3.3.2 Integration of Homophilous Graph Reconstruction and Existing Approaches. In the previous section, we show the importance of graph homophily. However, the experiments use ground-truth labels to change the level of graph homophily, which is not practical. Instead, we adapt three kinds of reconstruction modules (denoted as **R1**, **R2** and **R3**) as introduced in Sec. 3.2 to LPM and NRGNN, and evaluate their performance in two heterophilous datasets under different noise ratios. In detail, we directly replace the computation of A' , and keep Y' and Y_{final} unchanged for LPM and NRGNN in Equation 1. For different reconstruction modules (**R1**, **R2** and **R3**), A' is replaced by Z in Equation 2, $Z^{(L)*}$ in Equation 4, or $\hat{Z}^{(L)}$ in Equation 5. Figure 3 summarizes the results of all the variants.

From the figures, we see that (1) The replacement of homophilous graph reconstruction modules can generally improve the performance of LPM and NRGNN in heterophilous datasets. (2) The reconstruction module **R1**, which is based on cosine similarity, only considers node representations learned by the GNN model, and employs a hard threshold to determine the existence of edges. It heavily relies on the selected GNN and the pre-set threshold. Consequently, it cannot provide consistent improvement for both LPM and NRGNN. (3) The reconstruction modules **R2** and **R3** can clearly enhance the performance of LPM and NRGNN. This is because they directly learn the graph structure. Interestingly, the overall performance of **R2** surpasses that of **R3**, suggesting that Z derived in a closed-form solution can better capture the true relations between nodes. To summarize, incorporating graph reconstruction with homophily can effectively enhance existing approaches for graph noise labels. Among the tested modules, the second reconstruction module computed by Equation 4 demonstrates the best overall performance. We will employ it in our following experiments.

4 LP4GLN: A SIMPLE YET EFFECTIVE METHOD

Based on the above empirical analysis, we have identified two key findings. First, graph homophily can mitigate label noise. Second, label propagation is a simple yet effective approach to rectify incorrect labels when graph homophily is high. These findings inspire us to utilize homophily graph reconstruction and label propagation, and propose a new approach LP4GLN against arbitrary heterophily and label noise.

4.1 Basic version

Assume we have a graph \mathcal{G} with arbitrary heterophily, and a set of clean labels Y_C and noisy labels Y_N . Our goal is to obtain the correct labels for both noisy and unlabeled nodes. As previously designed, we first reconstruct the graph structure explicitly and compute the matrix $Z^{(L)*}$ by Equation 4. Simultaneously, the node representation $H^{(L)}$ is obtained. The training of the reconstruction module relies on the clean labels Y_C , which allows us to establish a mapping from $H^{(L)}$ to Y to generate the predicted labels Y_P for all unlabeled nodes. While Y_P is noisy, it still contains rich correct labels that are useful in label propagation.

Label propagation [31, 34] is a graph-based method to propagate label information across connected nodes. The fundamental assumption of LP is label smoothness, which posits that two connected nodes tend to share the same label. Thus, propagating existing labeled data (including clean/noisy/predicted labels) throughout the graph can effectively help us rectify noisy labels and assign appropriate labels to previously unlabeled nodes.

Here we set the similarity graph $S = Z^{(L)*}$, and $F \in \mathbb{R}^{n \times c}$ as the soft label matrix for nodes. When $t = 0$, we establish the initial label matrix $F(0) = \alpha_2 Y_C + \alpha_3 Y_N + \alpha_4 Y_P$. Note that in addition to the clean labels Y_C , both Y_N and Y_P could be noise-corrupted. Hence, we introduce three hyper-parameters α_2 , α_3 and α_4 to control the reliability of these initial labels. After that, in the t -th iteration, LP can be formulated as:

$$F(t+1) = \alpha_1 S F(t) + \alpha_2 Y_C + \alpha_3 Y_N + \alpha_4 Y_P, \quad (6)$$

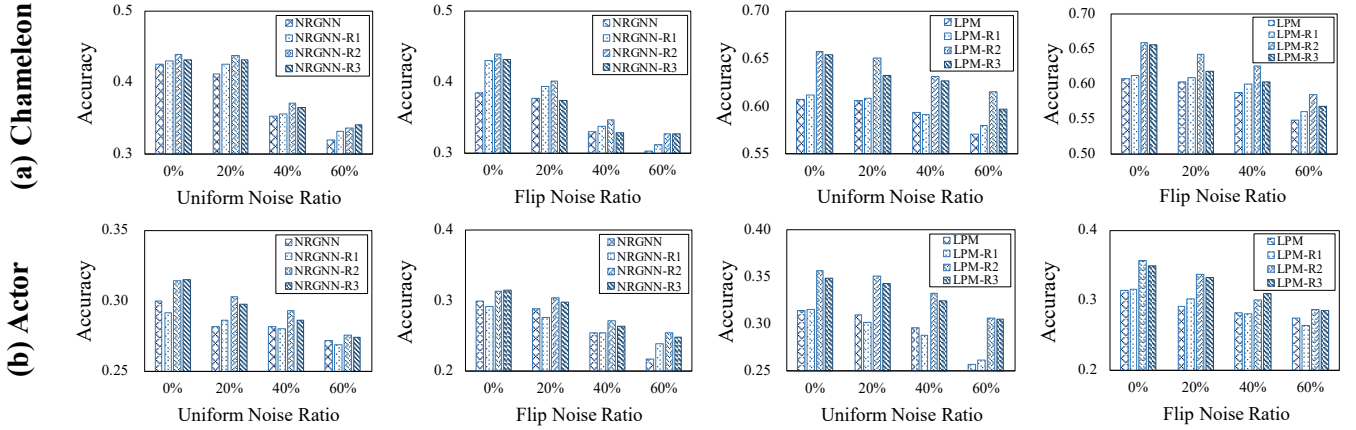


Figure 3: The performance of LPM and NRGNN incorporated with three graph reconstruction modules

where $\sum_{j=1}^4 \alpha_j = 1$ and each $\alpha_j \in [0, 1]$. With iterations in Equation 6, we derive:

$$F(t) = (\alpha_1 S)^{t-1} F(0) + \alpha_2 \sum_{i=0}^{t-1} (\alpha_1 S)^i Y_C + \alpha_3 \sum_{i=0}^{t-1} (\alpha_1 S)^i Y_N + \alpha_4 \sum_{i=0}^{t-1} (\alpha_1 S)^i Y_P. \quad (7)$$

Hence, we can also have a closed-form solution:

$$F^* = \lim_{t \rightarrow \infty} F(t) = (I - \alpha_1 S)^{-1} (\alpha_2 Y_C + \alpha_3 Y_N + \alpha_4 Y_P). \quad (8)$$

4.2 Efficiency Improvement

Directly calculating F^* by Equation 8 is computationally infeasible due to the cubic time complexity involved in computing $Z^{(L)*}$ in Equation 4 and the inverse term $(I - \alpha_1 S)^{-1}$. However, even quadratic time complexity is still high for large graph datasets. Therefore, we aim to accelerate the whole computation to achieve linear time complexity.

First of all, we utilize the Woodbury formula [23] to replace the inverse and transform Equation 4 into:

$$Z^{(L)*} = \left[(1 - \gamma) H^{(L)} (H^{(L)})^\top + \beta_2 \sum_{k=1}^K \lambda_k \hat{A}^k - \gamma (1 - \gamma) H^{(0)} (H^{(L)})^\top \right] \cdot \left[\frac{1}{\beta_1 + \beta_2} I_n - \frac{1}{(\beta_1 + \beta_2)^2} H^{(L)} \left[\frac{1}{(1 - \gamma)^2} I_d + \frac{1}{\beta_1 + \beta_2} (H^{(L)})^\top H^{(L)} \right]^{-1} (H^{(L)})^\top \right]^{-1} (H^{(L)})^\top \quad (9)$$

After that, we use first-order Taylor expansion and derive

$$F^* = (I - \alpha_1 S)^{-1} F(0) \approx (I + \alpha_1 S) F(0). \quad (10)$$

The inverse term in Equation 9 is computed on a matrix in $\mathbb{R}^{d \times d}$, whose time complexity is only $O(d^3)$. In this way, the overall time complexity of computing $Z^{(L)*}$ is $O(n^2)$, leading to a quadratic time complexity of calculating F^* in Equation 10.

Next, we combine Equations 9 and 10:

$$F^* = F(0) + \alpha_1 \left[(1 - \gamma) H^{(L)} (H^{(L)})^\top + \beta_2 \sum_{k=1}^K \lambda_k \hat{A}^k - \gamma (1 - \gamma) H^{(0)} (H^{(L)})^\top \right] Q, \quad (11)$$

where

$$Q = \frac{1}{\beta_1 + \beta_2} F(0) - \frac{1}{(\beta_1 + \beta_2)^2} H^{(L)} \cdot \left[\frac{1}{(1 - \gamma)^2} I_d + \frac{1}{\beta_1 + \beta_2} (H^{(L)})^\top H^{(L)} \right]^{-1} (H^{(L)})^\top F(0). \quad (12)$$

In this way, we avoid computing $Z^{(L)*}$ and $(I + \alpha_1 S)$ explicitly, and it can be further accelerated by matrix multiplication reordering. We first calculate Q in a right-to-left manner. Due to the time complexity $O(d^3)$ of computing the inverse term, the overall time complexity of calculating Q is $O(ncd + d^3)$, where $cd \ll n$ in the large datasets. After that, we calculate F^* in Equation 11 in a similar right-to-left manner. For example, for the term $H^{(0)} (H^{(L)})^\top Q$, we first compute $(H^{(L)})^\top Q$. Then we left-multiply the result with $H^{(0)}$, leading to a time complexity of $O(ncd)$. When computing the term $\sum_{k=1}^K \lambda_k \hat{A}^k Q$, we first calculate $\hat{A} Q$. Due to the sparsity of \hat{A} , the time complexity is $O(pcn)$, where p is the average number of non-zero entries in each row of \hat{A} . The total time complexity for $\sum_{k=1}^K \lambda_k \hat{A}^k Q$ is $O(Kpcn)$, where Kpc is a coefficient. Finally, we approximate the optimal label propagation results in a linear time.

4.3 Effectiveness Enhancement

To further enhance the effectiveness of LP4GLN, we employ a multi-round selection strategy. Specifically, F^* is obtained after the computation of graph reconstruction and label propagation. We then calculate the confidence based on F^* for noisy nodes, select the rectified nodes with the highest confidence and add them to the clean label set Y_C . In each time, $\varepsilon * |\mathcal{N}|$ nodes are chosen, where ε is the pre-set ratio. The updated clean label set can be leveraged in the next round to reconstruct the graph and refine the remaining nodes. Finally, we obtain an augmented clean label set, upon which we train a GNN classifier to obtain the node classification result. The pseudo-code of LP4GLN is provided in Appendix C.

4.4 Theoretical Verification

In this section, we theoretically analyze the denoising effect of label propagation. For clarity, we first assume the clean label is corrupted by a noise transition matrix $T \in [0, 1]^{c \times c}$, where $T_{ij} =$

$\mathbb{P}(\tilde{Y} = C_j | Y = C_i)$ is the probability of the label C_i being corrupted into the label C_j . For simplicity and following [22], we assume the classification is binary and the noise transition matrix is $T = \begin{bmatrix} 1-e & e \\ e & 1-e \end{bmatrix}$. After label propagation, the propagated label of the node v_i becomes a random variable

$$\hat{Y}_i = (1-\alpha)\tilde{Y}_i + \frac{\alpha}{d} \sum_{v_j \in \mathcal{N}_i} \tilde{Y}_j. \quad (13)$$

which is decided by its own noisy label \tilde{Y}_i and its d neighbors' noisy labels \tilde{Y}_j . We establish the following theorem for the propagated label \hat{Y}_i , and the detailed proof can be found in Appendix E.1.

Theorem 1. (*Label Propagation and Denoising*) *Suppose the label noise is generated by T and the label propagation follows Equation 13. For a specific node i , we further assume the node has d neighbors, and its neighbor nodes have the probability p to have the same true label with node i , i.e., $\mathbb{P}[Y_i = Y_j] = p$. After one-round label propagation, the gap between the propagated label and the ground-true label is:*

$$\begin{aligned} \mathbb{E}(Y - \hat{Y})^2 &= \mathbb{P}(Y = 0)\mathbb{E}(\hat{Y}|Y = 0)^2 \\ &+ \mathbb{P}(Y = 1)\left(\mathbb{E}(\hat{Y}|Y = 1) - 1\right)^2 + \text{Var}(\hat{Y}), \end{aligned} \quad (14)$$

where we have

$$\mathbb{E}(\hat{Y}|Y = 0) = (1-\alpha)e + \alpha[pe + (1-p)(1-e)], \quad (15a)$$

$$\mathbb{E}(\hat{Y}|Y = 1) = (1-\alpha)(1-e) + \alpha[p(1-e) + (1-p)e], \quad (15b)$$

$$\begin{aligned} \text{Var}(\hat{Y}) &= (1-\alpha)^2 e(1-e) \\ &+ \frac{\alpha^2}{d} [pe + (1-p)(1-e)][1-pe - (1-p)(1-e)]. \end{aligned} \quad (15d)$$

(1) **Heterophily and the impact of p :** In Equation 14, p plays the central role as a larger p can reduce all three terms in the bound. The value of p is related to the heterophily of a specific node and a more heterophilous node tends to have a smaller p . This is our major motivation to construct $Z^{(L)*}$ in the algorithm, which attempts to connect the nodes from the same class.

(2) **Label denoising effect:** We consider two special cases to see the label denoising by propagation. When we set $\alpha = 0$ and do not propagate the labels, $\mathbb{E}(Y - \hat{Y})^2 = \mathbb{E}(Y - Y)^2 = e$. When we set $p \rightarrow 1$ where all the neighbors have the same true labels, we have $\mathbb{E}(Y - \hat{Y})^2 \approx e^2 + \frac{1}{d}e(1-e)$, which is strictly less than e . It demonstrates the importance of neighbors. Besides, when we have more neighbors, the distance becomes smaller. It is the reason that $Z^{(L)*}$ is dense so each node could have more neighbors.

(3) **The impact of clean and predicted labels:** The bound in Equation 14 monotonically decreases with e and therefore having clean nodes can substantially reduce the bound. When the predicted labels are present, we have a larger number of neighbors for propagation, which also increases the value d .

In the following theorem, we analyze the generalization error of the final GNN classifier \hat{f} . The proof is provided in Appendix E.2.

Theorem 2. (*Generalization Error and Oracle Inequality*) *Denote the node feature X sampled from the distribution D , the graph topology as A , the set of training nodes as S_n , the graph neural network as $f(\cdot, \cdot)$, and the learned GNN classifier $\hat{f} = \inf_f \sum_{X \in S_n} (\hat{Y} - f(X, A))$.*

Suppose that the propagated label concentrated on its mean, i.e., with probability at least $\frac{\delta}{2}$, $\|\hat{Y} - Y\| - \mathbb{E}|\hat{Y} - Y| \leq \epsilon_1$. We further assume the generalization error is bounded with respect to the propagated labels, i.e., with probability at least $\frac{\delta}{2}$,

$$\mathbb{E}_{X \sim D} |\hat{Y} - \hat{f}(X, A)| - \inf_f \mathbb{E}_{X \sim D} |\hat{Y} - f(X, A)| \leq \epsilon_2.$$

Then we obtain the generalization error bound for training with noisy labels and test on the clean labels, i.e., with probability at least δ , the generalization error trained with propagated labels is given by

$$\mathbb{E}_{X \sim D} |Y - \hat{f}(X, A)| \leq \inf_f \mathbb{E}_{X \sim D} |Y - f(X, A)| + \epsilon_2 + 2(\mathbb{E}|\hat{Y} - Y| + \epsilon_1).$$

The generalization error mainly depends on ϵ_2 and $\mathbb{E}|\hat{Y} - Y|$. Our algorithm iteratively rectifies the noisy labels and selects high-confidence labels into the clean set, thereby reducing $\mathbb{E}|\hat{Y} - Y|$. In addition, as shown in [5], using the predicted labels generated by the same neural network is able to decrease ϵ_2 . This is the reason for the inclusion of predicted labels within our algorithm.

5 RELATED WORK

5.1 Deep Learning with Noisy Labels

Dealing with noisy labels can be approached through two main-stream directions: loss adjustment and sample selection [19]. Particularly, loss adjustment aims to mitigate the negative impact of noise by adjusting the loss value or the noisy labels. For example, [17] explicitly estimates the noise transition matrix to correct the forward and backward loss. Other effective techniques, such as [9, 18], refurbish the noisy labels by a convex combination of noisy and predicted labels. Sample selection, on the other hand, involves selecting true-labeled examples from a noisy training set via multi-network or multi-round learning. For instance, Co-teaching [7] and Co-teaching+ [29] use multi-network training, where two deep neural networks are maintained and each network selects a set of small-loss examples and feeds them to its peer network. Multi-round learning methods [18, 26] iteratively refine the selected set of clean samples by repeating the training rounds. As a result, the performance improves as the number of clean samples increases.

5.2 Learning GNNs with Noisy Labels

Graph neural networks (GNNs) [6, 11, 12, 21, 24, 28] have emerged as revolutionary technologies for graph-structured data, which can effectively capture complex patterns based on both node features and structure information, and then infer the accurate node labels. It is also common that real-world graphs are heterophilous which node is more likely to be connected with neighbors that have dissimilar features or different labels. Many studies are proposed to design GNNs for graphs with heterophily [1, 2, 15, 32].

The robustness of GNNs is well-studied, but most of them focus on the perturbation of graph structure and node features [4, 20, 25, 36] while few works study the label noise. NRGNN [3] and LPM [27] are the first two to deal with the label noise in GNNs explicitly. In detail, NRGNN generates pseudo labels and assigns more edges between unlabeled nodes and (pseudo) labeled nodes against label noise. LPM utilizes label propagation to aggregate original labels and pseudo labels to correct the noisy labels. However, they are only suitable for homophilous graphs, and perform badly on graphs

Table 1: The classification accuracy (%) over the methods on 10 datasets with flip noise ranging from 0% to 60%. We highlight the best score on each dataset in bold.

Types	Methods	Noise	Cora	Citeseer	Chameleon	Cornell	Wisconsin	Texas	Actor	Penn94	arXiv-year	snap-patents	
GNNs	GCN	0%	87.75	76.81	56.95	61.89	63.92	62.16	31.27	80.76	44.67	53.59	
		20%	86.08	75.48	56.27	60.00	62.94	61.89	30.63	78.99	40.93	49.49	
		40%	81.30	70.99	53.81	60.27	61.17	61.35	26.38	75.84	40.20	41.84	
		60%	53.85	42.94	52.98	49.18	36.47	48.64	21.51	72.70	38.73	30.55	
	GloGNN	0%	84.57	76.09	68.83	83.51	88.43	84.05	38.55	85.66	52.74	62.33	
		20%	80.84	74.09	67.76	76.48	81.76	71.62	37.55	76.97	47.67	54.72	
		40%	37.55	63.54	63.00	70.27	74.31	61.08	33.64	62.55	36.93	38.74	
		60%	75.10	40.17	55.08	52.43	56.86	53.78	30.31	51.79	25.45	26.37	
	H ₂ GCN	0%	87.87	77.11	60.01	82.59	85.65	86.26	35.70	79.02	48.72	57.21	
		20%	83.51	74.80	54.10	74.45	71.96	70.78	32.49	74.08	43.20	52.06	
		40%	82.00	71.42	47.82	65.67	70.60	67.83	29.73	67.42	36.57	46.23	
		60%	81.36	71.23	34.51	55.27	64.90	60.81	30.21	54.47	29.81	38.57	
Methods for Label Noise	Co-teaching+	0%	85.76	76.10	72.52	70.54	72.49	67.91	34.28	86.90	OOM	OOM	
		20%	68.79	70.19	66.09	66.09	61.92	64.70	30.16	77.68	OOM	OOM	
		40%	55.34	47.87	41.03	41.03	57.88	57.08	24.98	61.82	OOM	OOM	
		60%	35.72	36.11	28.57	28.57	39.60	38.56	21.16	50.18	OOM	OOM	
	Backward	0%	84.88	77.06	71.00	72.70	81.37	84.31	23.90	87.00	46.51	58.54	
		20%	81.04	72.43	67.69	69.72	75.88	74.72	21.15	80.84	40.29	56.30	
		40%	71.28	62.03	61.73	68.91	63.13	60.78	20.01	70.00	32.24	43.61	
		60%	56.70	48.37	53.15	51.35	45.49	53.51	20.09	51.57	26.21	31.57	
	Methods for Graph Label Noise	NRGNN	0%	82.87	72.52	38.50	69.91	69.17	72.64	28.82	68.31	OOM	OOM
			20%	82.30	72.47	37.83	61.70	67.37	70.32	28.75	66.80	OOM	OOM
40%			79.13	67.42	33.09	54.59	61.64	57.02	25.40	63.59	OOM	OOM	
60%			75.40	60.00	30.35	42.70	58.23	54.59	21.69	53.14	OOM	OOM	
LPM		0%	89.74	78.77	60.72	63.87	73.72	69.46	31.43	76.10	44.32	56.76	
		20%	86.55	75.92	60.31	62.21	72.35	68.10	29.11	75.35	42.03	53.84	
		40%	83.97	72.62	58.77	61.35	70.78	67.02	28.52	71.45	38.46	48.36	
		60%	80.47	68.72	54.75	58.37	64.11	62.16	27.51	63.14	32.11	40.21	
LP4GLN		0%	87.69	78.09	73.05	87.84	88.82	87.30	38.59	86.78	53.80	63.04	
		20%	86.85	76.30	68.38	84.32	86.86	83.24	37.37	82.69	50.11	58.59	
	40%	85.00	74.41	61.23	77.84	83.14	77.02	35.86	79.05	46.19	55.90		
	60%	82.53	72.73	57.46	71.35	75.68	69.46	35.08	77.09	46.11	52.71		

with heterophily. Our proposed approach, LP4GLN relaxes the homophily assumption and is more resilient to various types of noise.

6 EXPERIMENTS

6.1 Experimental Settings

Datasets. We conduct experiments on 10 benchmark datasets, which include 2 homophilous graphs (Cora, Citeseer), 5 heterophilous graphs (Chameleon, Cornell, Wisconsin, Texas, Actor) and 3 large-scale heterophilous graphs (Penn94, arXiv-year, snap-patent). For each dataset, we randomly split nodes into 60%, 20%, and 20% for training, validation and testing, and measure the performance of all models on the test set. The statistics and details of these datasets can be found in Appendix A.

Label noise. We set 10% nodes with clean labels, and corrupt the remaining training nodes with noise in training set. Following [17], We consider two types of noise: *uniform noise* means the true label c_i have a probability e to be uniformly flipped to other classes, i.e. $T_{ij} = e/(c-1)$ for $i \neq j$ and $T_{ii} = 1 - e$; *flip noise* means the true

label C_i have a probability e to be flipped to only a similar class C_j , i.e. $T_{ij} = e$ and $T_{ii} = 1 - e$. We varied the value of e from 0% to 60%.

Baselines. We compare LP4GLN with 7 baselines, which can be categorized into three types. The first type involves (1) **GCN** [11] (2) **GloGNN** [15] and (3) **H₂GCN** [32], three popular GNNs for homophilous and heterophilous graphs. They are directly trained on both clean and noisy training samples. In the second type, we compare with two GNNs dealing with label noise, including (4) **NRGNN** [3] and (5) **LPM** [27]. In detail, NRGNN assigns more edges between unlabeled nodes and (pseudo) labeled nodes against noise. LPM addresses the graph label noise by label propagation and meta-learning. In the third type, we modify two typical loss correction and sample selection methods and make them suitable for graph data. (6) **Co-teaching+** [29] is a multi-network training method to select clean samples. (7) **Backward** [17] is to revise predictions and obtain unbiased loss on noisy training samples. For fairness, we use GloGNN as a backbone GNN model for Co-teaching+ and Backward.

Other materials. Due to the space limitation, we move the experimental setup (Sec. A), dataset descriptions (Sec. B), hyper-parameter

sensitivity analysis (Sec. D.2), and the ablation study with/without a clean label set (Sec. D.3) to Appendix.

6.2 Performance Results

Table 1 presents the performance results of all the methods on 10 benchmark datasets under different flip noise levels. We attach the Table 5 for various uniform noise levels in Appendix. Every method was repeated 10 times for small-scale datasets and 5 times for large-scale datasets over different random splits, and we report the mean classification accuracy on the test set. From the tables, we make the following observations: (1) LP4GLN consistently outperforms the competitive methods across various noise settings in the majority of cases. (2) The GNN models GCN, GloGNN and H₂GCN exhibit good performance on homophilous graphs. However, their accuracy drops dramatically as the noise ratio increases on heterophilous graphs. (3) LPM and NRGNN aim to address the label noise in graphs, but their accuracy is limited on heterophilous graphs because they rely on the assumption of graph homophily and label smoothness. (4) Co-teaching+ and Backward are two mainstream methods to address the label noise through sample selection and loss correction. However, their accuracy significantly declines when facing a high noise ratio.

Overall, LP4GLN iteratively learns graph homophily to correct noise labels, ensures high-quality labels for training the GNN model, and achieves high and stable accuracy under different noises.

6.3 Ablation Study

The ablation study is done to understand the main components of LP4GLN. We first remove the whole label propagation step and call this variant LP4GLN-nlp (no label propagation step). Instead, we use self-training [14] that just pick the most confident noisy labels in the GNN and put them into the clean set to improve the performance. Secondly, we replace the reconstructed graph with the similarity matrix and call this variant LP4GLN-nz (no $Z^{(l)*}$). Further, we do not propagate the noisy labels or the predicted labels in the label propagation, respectively, and call these two variants LP4GLN-nnl (no noisy labels) and LP4GLN-npl (no predicted labels). We compare LP4GLN with these four variants, and the results are presented in Figure 4. Our findings show that LP4GLN outperforms all the variants on the two datasets. Furthermore, the performance gap between LP4GLN and LP4GLN-nlp highlights the importance of label propagation for label correction. The noise labels significantly enhance the performance of label propagation, especially on heterophilous graphs.

6.4 Analysis of Selection Strategies

We compare the performance of LP4GLN by using different selection functions: (1) *Threshold* [29] chooses the noisy labels whose confidence is greater than a certain threshold; (2) *Absolute number* selects an absolute number of noisy labels with high confidence based on the current number of samples; (3) *Statistical selection* [16] uses statistics to derive the threshold for sample selection; (4) LP4GLN selects samples with high confidence based on a certain proportion relative to the current noisy nodes. Figure 5 shows the results on Cora and Chameleon datasets. From the figures, we observe that the accuracy drops dramatically as the noise ratio

increases when using *Threshold* and *Absolute number*. The reason is that they choose many noisy labels into the clean set. *Statistical selection* accurately selects the node labels, but too stringent selection conditions limit the number of selected labels. Compared with these functions, LP4GLN selects the labels with respect to the suitable quantity and high quality of remaining samples.

7 CONCLUSION

In this paper, we address the problem of graph label noise under arbitrary graph heterophily. We begin by empirically exploring the relationship between graph homophily and label noise, leading to two key observations: (1) graph homophily can indeed mitigate graph label noise, and (2) LP-based methods achieve great performance as graph homophily increases. These findings inspire us to combine LP with homophilous graph reconstruction to propose a simple yet effective algorithm LP4GLN. It is a multi-round process that performs graph reconstruction with homophily, label propagation for noisy label refinement and high-confidence sample selection iteratively. Finally, we conducted extensive experiments and demonstrated the superior performance of LP4GLN compared to other 7 state-of-the-art competitors on 10 benchmark datasets. In the future, we plan to explore and improve LP4GLN in more challenging scenarios, where the clean label set is unavailable, or input data, including node features and graph topology, also exhibits noise.

REFERENCES

- [1] Deyu Bo, Xiao Wang, Chuan Shi, and Huawei Shen. 2021. Beyond Low-frequency Information in Graph Convolutional Networks. In AAAI. AAAI Press.
- [2] Eli Chien, Jianhao Peng, Pan Li, and Olga Milenkovic. 2021. Adaptive Universal Generalized PageRank Graph Neural Network. In *International Conference on Learning Representations*. <https://openreview.net/forum?id=n6jl7fLxrP>
- [3] Enyan Dai, Charu Aggarwal, and Suhang Wang. 2021. Nrgnn: Learning a label noise resistant graph neural network on sparsely and noisily labeled graphs. In *Proceedings of the 27th ACM SIGKDD Conference on Knowledge Discovery & Data Mining*. 227–236.
- [4] Hanjun Dai, Hui Li, Tian Tian, Xin Huang, Lin Wang, Jun Zhu, and Le Song. 2018. Adversarial attack on graph structured data. In *International conference on machine learning*. PMLR, 1115–1124.
- [5] Bin Dong, Jikai Hou, Yiping Lu, and Zhihua Zhang. 2019. Distillation *approx* Early Stopping? Harvesting Dark Knowledge Utilizing Anisotropic Information Retrieval For Overparameterized Neural Network. *arXiv preprint arXiv:1910.01255* (2019).
- [6] Will Hamilton, Zitao Ying, and Jure Leskovec. 2017. Inductive representation learning on large graphs. 1024–1034.
- [7] Bo Han, Quanming Yao, Xingrui Yu, Gang Niu, Miao Xu, Weihua Hu, Ivor Tsang, and Masashi Sugiyama. 2018. Co-teaching: Robust training of deep neural networks with extremely noisy labels. *Advances in neural information processing systems* 31 (2018).
- [8] Aidan Hogan, Eva Blomqvist, Michael Cochez, Claudia d’Amato, Gerard De Melo, Claudio Gutierrez, Sabrina Kirrane, José Emilio Labra Gayo, Roberto Navigli, Sebastian Neumaier, et al. 2021. Knowledge graphs. *ACM Computing Surveys (Csur)* 54, 4 (2021), 1–37.
- [9] Lang Huang, Chao Zhang, and Hongyang Zhang. 2020. Self-adaptive training: beyond empirical risk minimization. *Advances in neural information processing systems* 33 (2020), 19365–19376.
- [10] Diederik P Kingma and Jimmy Ba. 2014. Adam: A method for stochastic optimization. *arXiv preprint arXiv:1412.6980* (2014).
- [11] Thomas N Kipf and Max Welling. 2017. Semi-supervised classification with graph convolutional networks.
- [12] Johannes Klicpera, Aleksandar Bojchevski, and Stephan Günnemann. 2019. Predict then Propagate: Graph Neural Networks meet Personalized PageRank.
- [13] Jure Leskovec, Daniel Huttenlocher, and Jon Kleinberg. 2010. Predicting positive and negative links in online social networks. In *Proceedings of the 19th international conference on World wide web*. 641–650.
- [14] Qimai Li, Zhichao Han, and Xiao-Ming Wu. 2018. Deeper insights into graph convolutional networks for semi-supervised learning. In *Proceedings of the AAAI*

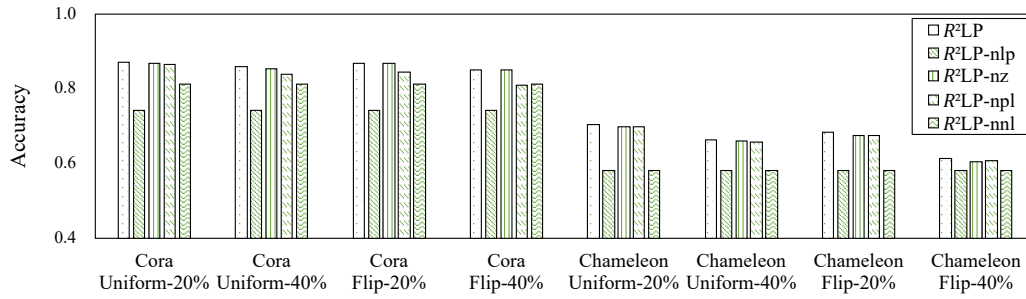


Figure 4: Ablation study on the main components of LP4GLN.

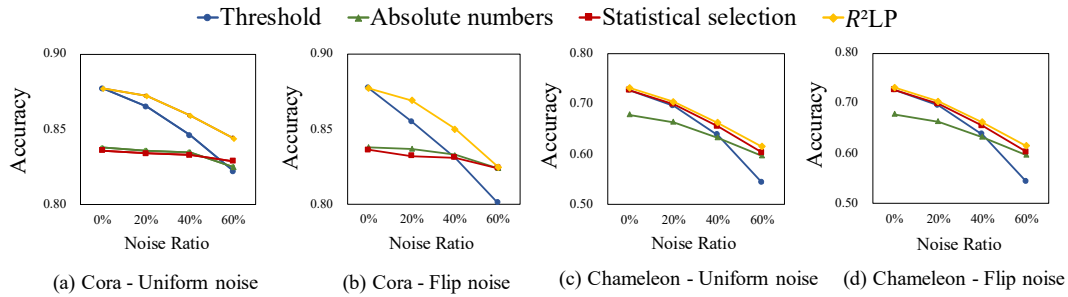


Figure 5: The effect of different selection strategies.

- conference on artificial intelligence, Vol. 32.
- [15] Xiang Li, Renyu Zhu, Yao Cheng, Caihua Shan, Siqiang Luo, Dongsheng Li, and Weining Qian. 2022. Finding global homophily in graph neural networks when meeting heterophily. In *International Conference on Machine Learning*. PMLR, 13242–13256.
- [16] Deep Patel and PS Sastry. 2023. Adaptive sample selection for robust learning under label noise. In *Proceedings of the IEEE/CVF Winter Conference on Applications of Computer Vision*. 3932–3942.
- [17] Giorgio Patrini, Alessandro Rozza, Aditya Krishna Menon, Richard Nock, and Lizhen Qu. 2017. Making deep neural networks robust to label noise: A loss correction approach. In *Proceedings of the IEEE conference on computer vision and pattern recognition*. 1944–1952.
- [18] Hwanjun Song, Minseok Kim, and Jae-Gil Lee. 2019. Selfie: Refurbishing unclean samples for robust deep learning. In *International Conference on Machine Learning*. PMLR, 5907–5915.
- [19] Hwanjun Song, Minseok Kim, Dongmin Park, Yooju Shin, and Jae-Gil Lee. 2022. Learning from noisy labels with deep neural networks: A survey. *IEEE Transactions on Neural Networks and Learning Systems* (2022).
- [20] Yiwei Sun, Suhang Wang, Xianfeng Tang, Tsung-Yu Hsieh, and Vasant Honavar. 2020. Adversarial attacks on graph neural networks via node injections: A hierarchical reinforcement learning approach. In *Proceedings of the Web Conference 2020*. 673–683.
- [21] Petar Veličković, Guillem Cucurull, Arantxa Casanova, Adriana Romero, Pietro Lio, and Yoshua Bengio. 2018. Graph attention networks.
- [22] Jiaheng Wei, Hangyu Liu, Tongliang Liu, Gang Niu, Masashi Sugiyama, and Yang Liu. 2021. To smooth or not? when label smoothing meets noisy labels. *Learning* 1, 1 (2021), e1.
- [23] M. Woodbury and M. Woodbury. 1950. Inverting modified matrices. (1950).
- [24] Felix Wu, Amauri Souza, Tianyi Zhang, Christopher Fifty, Tao Yu, and Kilian Weinberger. 2019. Simplifying graph convolutional networks. PMLR, 6861–6871.
- [25] Huijun Wu, Chen Wang, Yuriy Tyshetskiy, Andrew Docherty, Kai Lu, and Liming Zhu. 2019. Adversarial examples on graph data: Deep insights into attack and defense. *arXiv preprint arXiv:1903.01610* (2019).
- [26] Pengxiang Wu, Songzhu Zheng, Mayank Goswami, Dimitris Metaxas, and Chao Chen. 2020. A topological filter for learning with label noise. *Advances in neural information processing systems* 33 (2020), 21382–21393.
- [27] Jun Xia, Haitao Lin, Yongjie Xu, Lirong Wu, Zhangyang Gao, Siyuan Li, and Stan Z Li. 2021. Towards robust graph neural networks against label noise. (2021).
- [28] Keyulu Xu, Weihua Hu, Jure Leskovec, and Stefanie Jegelka. 2018. How powerful are graph neural networks?
- [29] Xingrui Yu, Bo Han, Jiangchao Yao, Gang Niu, Ivor Tsang, and Masashi Sugiyama. 2019. How does disagreement help generalization against label corruption?. In *International Conference on Machine Learning*. PMLR, 7164–7173.
- [30] Chiyuan Zhang, Samy Bengio, Moritz Hardt, Benjamin Recht, and Oriol Vinyals. 2021. Understanding deep learning (still) requires rethinking generalization. *Commun. ACM* 64, 3 (2021), 107–115.
- [31] Dengyong Zhou, Olivier Bousquet, Thomas Lal, Jason Weston, and Bernhard Schölkopf. 2003. Learning with local and global consistency. *Advances in neural information processing systems* 16 (2003).
- [32] Jiong Zhu, Yujun Yan, Lingxiao Zhao, Mark Heimann, Leman Akoglu, and Danai Koutra. 2020. Beyond homophily in graph neural networks: Current limitations and effective designs. *Advances in Neural Information Processing Systems* 33 (2020), 7793–7804.
- [33] Jiong Zhu, Yujun Yan, Lingxiao Zhao, Mark Heimann, Leman Akoglu, and Danai Koutra. 2020. Beyond homophily in graph neural networks: Current limitations and effective designs. *Advances in Neural Information Processing Systems* 33 (2020), 7793–7804.
- [34] Xiaojin Zhu. 2005. *Semi-supervised learning with graphs*. Carnegie Mellon University.
- [35] Marinka Zitnik and Jure Leskovec. 2017. Predicting multicellular function through multi-layer tissue networks. *Bioinformatics* 33, 14 (2017), i190–i198.
- [36] Daniel Zügner, Amir Akbarnejad, and Stephan Günnemann. 2018. Adversarial attacks on neural networks for graph data. In *Proceedings of the 24th ACM SIGKDD international conference on knowledge discovery & data mining*. 2847–2856.

A EXPERIMENTAL SETUP

We implemented LP4GLN by PyTorch and conducted the experiments on 10 datasets with one A100 GPU. The model is optimized by Adam [10]. To fine-tune hyperparameters, we performed a grid search based on the result of the validation set. Table 3 summarizes the search space of hyper-parameters in LP4GLN.

B DATASET DESCRIPTION

In this section, we introduce the datasets used in the experiments. The statistics of datasets are listed in Table 2, and we describe each dataset in detail below:

Cora and Citeseer are two graphs commonly used as benchmarks. In these datasets, each node represents a scientific paper and each edge represents a citation. Bag-of-words representations serve as feature vectors for each node. The label of nodes indicates the research field of the paper.

Texas, Wisconsin and Cornell are three heterophilous graphs representing links between web pages at the corresponding universities. In these datasets, each node represents a web page and each edge represents a hyperlink between nodes. Bag-of-words representations are also used as feature vectors for each node. The label is the web category.

Chameleon is a subgraph of web pages in Wikipedia, and the task is to classify nodes into five categories.

Actor is a heterophilous graph that represents actor co-occurrence in Wikipedia pages. Each node represents the actor, and each edge is the co-occurrence in Wikipedia pages. Node features are derived from keywords included in the actor’s Wikipedia page. The task is to categorize actors into five classes.

Penn94 is a subgraph extracted from Facebook whose nodes are students. Node features include major, second major/minor, dorm/house, year and high school. We take students’ genders as nodes’ labels.

arXiv-year and snap-patents are two heterophilous citation networks. *arXiv-year* is a directed subgraph of ogbn-arXiv, where nodes are arXiv papers and edges represent the citation relations. We construct node features by taking the averaged word2vec embedding vectors of tokens contained in both the title and abstract of papers. The task is to classify these papers into five labels that are constructed based on their posting year. *snap-patents* is a US patent network whose nodes are patents and edges are citation relations. Node features are constructed from patent metadata. Our goal is to classify the patents into five labels based on the time when they were granted.

C PSEUDO CODE

We summarize the pseudo-code of LP4GLN in Algorithm 1. The input is a graph with the topology A and node features X , and we divide the nodes into three sets C , \mathcal{N} and \mathcal{U} . Here, C represents clean labeled nodes, \mathcal{N} denotes noisy labeled nodes, and \mathcal{U} represents unlabeled nodes. We have the labels Y_C and $Y_{\mathcal{N}}$, and we aim to predict $Y_{\mathcal{U}}$. The whole process is a multi-round training to select the noisy nodes with corrected labels into the clean node set C . In each round, we first reconstruct the graph with homophily based on the current clean labels, and train a GNN to obtain the predicted labels for all the nodes as extra information. Next, we employ label propagation to rectify noisy labels. Given the selection

Algorithm 1: LP4GLN

Input: Graph $\mathcal{G} = (\mathcal{V}, A, X)$, $\mathcal{V} = C \cup \mathcal{N} \cup \mathcal{U}$, Y_C , $Y_{\mathcal{N}}$, multi-round epoch T , selection ratio ϵ .
Output: The label of unlabeled nodes $Y_{\mathcal{U}}$.

- 1 **for** $t = 0, 1, \dots, T - 1$ **do**
- 2 Generate $Z^{(L)*}$ on C by Eq. 4
- 3 Train a GNN on $Z^{(L)*}$ and C and calculate the predicted labels $Y_{\mathcal{P}}$ for all the nodes
- 4 Utilize the label propagation to rectify noisy labels by Eq. 11
- 5 select $\epsilon|\mathcal{N}|$ nodes from \mathcal{N} based on the confidence of F^* , and then transfer them from \mathcal{N} to C
- 6 Train a GNN on the final clean set C , and obtain the predicted labels $Y_{\mathcal{U}}$
- 7 **return** $Y_{\mathcal{U}}$

ratio ϵ , we select a portion of the current noisy nodes based on the confidence of F^* . Lastly, we transfer the selected noisy nodes with their corrected labels from \mathcal{N} to C and initiate a new round. After we end all the rounds, we obtain the final clean set C to train a GNN and predict the labels for unlabeled nodes.

D ADDITIONAL EXPERIMENTAL RESULT

D.1 Graph Homophily Mitigates Graph Label Noise

We conducted experiments on 4 existing methods, including two SOTA methods for graph label noise: LPM and NRGNN; and two classical methods: GCN and LP. Figure 7 shows the performance of all the methods under different levels of uniform label noise.

D.2 Sensitivity Analysis.

Here we study the sensitivity of four hyper-parameters: the weight $\alpha_1, \alpha_2, \alpha_3$ and the sample selection ratio ϵ . The results are shown in Figure 6. For all the hyper-parameters, LP4GLN consistently performs well across a wide range of values, which demonstrates that these hyper-parameters do not significantly impact the performance of LP4GLN.

D.3 Performance without Clean Set.

We evaluate the performance of LP4GLN when no clean nodes set is available, i.e., all the node labels are corrupted by noise. Specifically, in the initial step, we do not train the GNN with clean labels to reconstruct a new graph with homophily. In other words, we use the random parameters to generate $H^{(0)}$, and then calculate $Z^{(L)*}$ accordingly. Table 4 presents the result on Cora and Chameleon with different noise settings. Surprisingly, the performance of LP4GLN does not decrease much when the noise ratio is low. This shows that the clean label set is not necessary under a small noise ratio. However, the classification accuracy dramatically drops with a high flip noise, which demonstrates the necessity of a small set of clean labels at a high noise rate.

Table 2: Datasets statistics. Note that Edge Hom. [33] is defined as the fraction of edges that connect nodes with the same label.

	Cora	Citeseer	Chameleon	Cornell	Wisconsin	Texas	Actor	Penn94	arXiv-year	snap-patents
Edge Hom.	0.81	0.74	0.23	0.30	0.21	0.11	0.22	0.47	0.22	0.07
#Nodes	2,708	3,327	2,277	183	251	183	7,600	41,554	169,343	2,923,922
#Edges	5,278	4,676	31,421	280	466	295	26,752	1,362,229	1,166,243	13,975,788
#Features	1,433	3,703	2,325	1,703	1,703	1,703	931	5	128	269
#Classes	7	6	5	5	5	5	5	2	5	5

Table 3: Grid search space.

Hyper-parameter	Search space
lr	{0.005, 0.01, 0.02, 0.03}
dropout	[0.0, 0.9]
weight decay	{1e-7, 5e-6, 1e-6, 5e-5, 1e-5, 5e-4}
α_1	[0.0, 1.0]
α_2	[0.0, 1.0]
α_3	[0.0, 1.0]
ϵ	[0.1, 0.9]

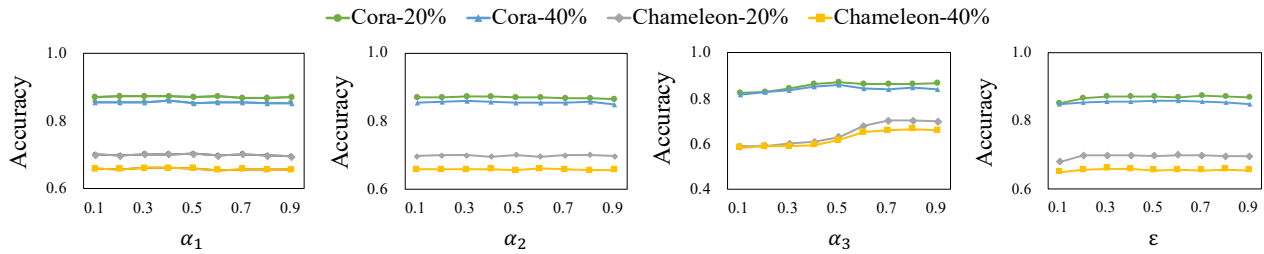


Figure 6: Hyper-parameter sensitivity analysis

Table 4: The classification accuracy (%) with/without a set of clean labels

Datasets	Methods	Uniform Noise			Flip Noise		
		20%	40%	60%	20%	40%	60%
Cora	LP4GLN	87.23	85.90	84.37	86.85	85.00	82.53
	without clean labels	85.45	84.32	78.87	84.95	76.21	46.62
Chameleon	LP4GLN	70.28	66.23	61.40	68.38	61.23	57.46
	without clean labels	69.45	64.16	58.13	67.23	59.01	42.87

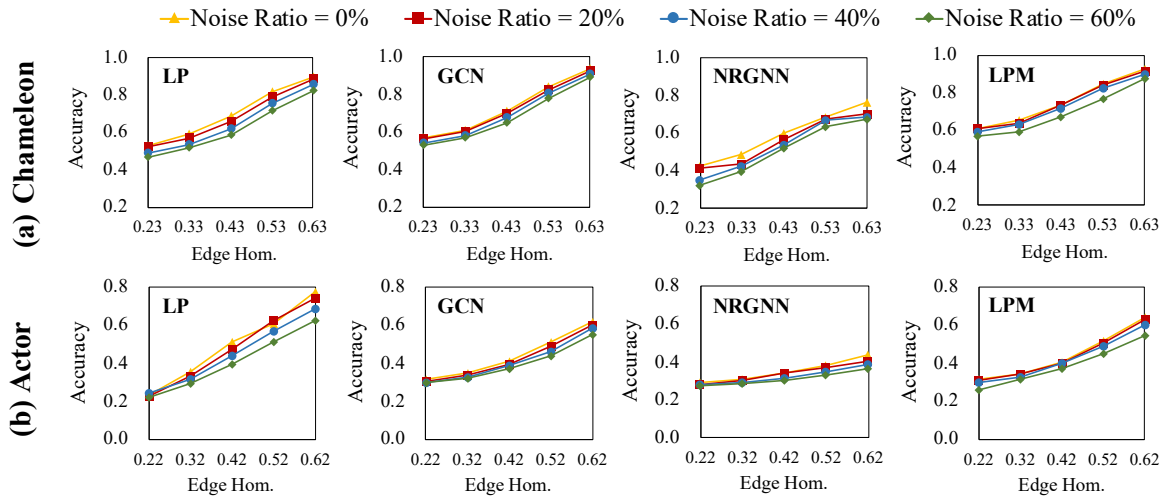


Figure 7: The impact of edge homophily on graph label noise across various methods (uniform noise)

Table 5: The classification accuracy (%) over the methods on 10 datasets with uniform noise ranging from 0% to 60%. We highlight the best score on each dataset in bold.

Types	Methods	Noise	Cora	Citeseer	Chameleon	Cornell	Wisconsin	Texas	Actor	Penn94	arXiv-year	snap-patents
GNNs	GCN	0%	87.75	76.81	56.95	61.89	63.92	62.16	31.27	80.76	44.67	53.59
		20%	86.54	75.66	54.29	61.08	63.52	62.43	30.27	80.29	39.59	50.89
		40%	85.74	75.05	48.90	61.08	60.19	62.43	30.08	78.21	38.17	48.39
		60%	83.67	73.44	33.13	60.54	60.78	61.62	29.79	76.74	36.88	46.81
	GloGNN	0%	84.58	76.09	69.83	83.51	88.43	84.05	38.55	85.66	52.74	62.33
		20%	82.53	74.64	69.38	80.81	84.31	80.00	37.86	81.85	50.47	58.96
		40%	79.92	72.62	65.78	74.86	74.50	68.37	37.33	77.44	47.77	54.97
		60%	75.70	69.90	61.55	69.45	66.27	61.89	36.06	71.59	44.82	50.12
	H ₂ GCN	0%	87.87	77.11	60.00	82.59	85.65	86.26	35.70	79.02	48.72	57.21
		20%	85.34	74.51	55.31	74.27	75.09	77.27	31.25	76.22	45.60	54.68
		40%	82.46	73.17	51.79	67.02	74.50	69.45	31.95	73.73	40.13	50.18
		60%	80.94	70.87	46.60	57.56	69.01	62.16	31.25	71.01	33.65	41.36
Methods for Label Noise	Co-teaching+	0%	85.76	76.32	72.52	70.54	72.68	67.21	34.56	86.90	OOM	OOM
		20%	80.46	73.32	67.30	69.91	60.19	64.56	33.62	82.73	OOM	OOM
		40%	70.00	63.00	58.81	54.05	54.05	60.70	30.27	73.86	OOM	OOM
		60%	59.17	52.29	51.90	49.18	43.72	43.24	27.06	52.03	OOM	OOM
	Backward	0%	84.88	77.06	71.00	72.70	81.37	84.31	23.90	87.00	46.51	58.54
		20%	83.35	75.52	69.34	68.91	75.68	76.07	22.13	84.34	43.85	56.41
		40%	80.18	69.89	65.76	68.64	71.72	70.78	22.98	80.90	33.16	56.37
		60%	76.16	67.20	61.93	58.37	66.66	67.19	21.28	76.71	27.80	52.25
Methods for Graph Label Noise	NRGNN	0%	84.14	73.93	42.64	69.91	70.80	72.64	28.95	68.31	OOM	OOM
		20%	82.73	72.94	41.17	68.84	68.62	71.05	28.24	67.02	OOM	OOM
		40%	80.66	63.88	35.26	61.37	58.17	61.75	28.15	65.89	OOM	OOM
		60%	73.67	62.95	31.97	58.19	50.39	57.56	27.24	53.60	OOM	OOM
	LPM	0%	89.74	78.77	60.72	63.87	73.72	69.46	31.43	76.10	44.32	56.76
		20%	87.06	78.24	60.57	62.70	72.15	69.19	30.95	75.62	42.15	54.13
		40%	84.81	74.50	59.38	62.43	69.21	68.11	29.62	73.50	39.44	50.27
		60%	81.42	70.97	57.10	62.16	67.84	63.78	25.71	69.98	35.41	44.36
	LP4GLN	0%	87.69	78.09	73.05	87.84	88.82	87.30	38.59	86.78	53.80	63.04
		20%	87.23	76.54	70.28	87.03	88.43	86.49	38.46	84.72	52.18	59.86
		40%	85.90	75.16	66.23	80.00	83.92	78.37	37.51	83.03	50.42	57.33
		60%	84.37	73.91	61.40	74.32	81.18	73.24	36.82	81.48	48.01	55.29

E PROOFS

E.1 Proof of Theorem 1

Remember we obtain the propagated label of the node i by $\hat{Y}_i = (1 - \alpha)\tilde{Y}_i + \frac{\alpha}{d} \sum_{j \in [d]} \tilde{Y}_j$. The first part is its own noisy label \tilde{Y}_i , and the second part is the label aggregation from its d neighbors' noisy labels \tilde{Y}_j . We first analyze the distribution of $Y^{\text{neighbor}} = \sum_{j \in [d]} \tilde{Y}_j$.

Theorem 3. *Assume that the true label of node i is $Y_i = 0$. Then the distribution of $Y^{\text{neighbor}} = \sum_{j \in [d]} \tilde{Y}_j$ follows a conditional binomial given by $Y^{\text{neighbor}} \sim B(d, pe + (1 - p)(1 - e))$. Similarly, when $Y_i = 1$, the distribution of Y^{neighbor} is also a conditional binomial $Y^{\text{neighbor}} \sim B(d, p(1 - e) + (1 - p)e)$.*

In both cases, the parameter d represents the number of neighbors, p means the probability of the neighbor having the same label as node i , and e represents the probability of an error in the labeling process, where $\Pr(\tilde{Y}_i = 1 | Y_i = 0) = e$ and $\Pr(\tilde{Y}_i = 0 | Y_i = 1) = e$.

PROOF. Let N_s be a random variable representing the number of neighbors that have the same true labels with the node i , where $0 \leq N_s \leq d$. The probability that $Y^{\text{neighbor}} = m$ can be expressed as the sum of conditional probabilities:

$$\Pr(Y^{\text{neighbor}} = m) = \sum_{i=0}^d \Pr(N_s = i) \Pr[Y^{\text{neighbor}} = m \mid N_s = i]$$

The case $Y^{\text{neighbor}} = m$ comes from two parts. The first part is that $Y^{\text{neighbor}} = j$ originates from the neighbor nodes that share the same true labels as node i . The second part is that $Y^{\text{neighbor}} = m - j$ comes from the neighbor nodes that have different true labels. Hence, the equation can be expressed as follows:

$$\begin{aligned} &= \sum_{i=0}^d \Pr(N_s = i) \left[\sum_{j=0}^{\min(i, m)} \Pr[Y^{\text{neighbor}} = j \text{ in } N_s, Y^{\text{neighbor}} = m - j \text{ not in } N_s] \right] \\ &= \sum_{i=0}^d \binom{d}{i} p^i (1 - p)^{d-i} \left[\sum_{j=0}^{\min(i, m)} \binom{i}{j} e^j (1 - e)^{i-j} \binom{d-i}{m-j} (1 - e)^{m-j} e^{d-i-m+j} \right] \\ &= \sum_{i=0}^d \binom{d}{i} p^i (1 - p)^{d-i} \left[\sum_{j=0}^{\min(i, m)} \binom{i}{j} \binom{d-i}{m-j} (1 - e)^{m+i-2j} e^{d-i-m+2j} \right] \\ &= \sum_{i=0}^d \sum_{j=0}^{\min(i, m)} \left[\binom{d}{i} \binom{i}{j} \binom{d-i}{m-j} p^i (1 - p)^{d-i} (1 - e)^{m+i-2j} e^{d-i-m+2j} \right] \\ &= \sum_{i=0}^d \sum_{j=0}^{\min(i, m)} \left[\frac{d!}{j!(i-j)!(m-j)!(d-i-m+j)!} p^i (1 - p)^{d-i} (1 - e)^{m+i-2j} e^{d-i-m+2j} \right] \end{aligned}$$

Let $a = i - j$ and $b = j$, we have $i = a + b$ and $j = b$. Because of $0 \leq i \leq d$, $0 \leq j \leq m$, $j \leq i$ and $i - j \leq d - m$, we can obtain $0 \leq a \leq d - m$ and $0 \leq b \leq m$. The above equation is rewritten as

$$\begin{aligned} &= \sum_{a=0}^{d-m} \sum_{b=0}^m \left[\frac{d!}{b!a!(m-b)!(d-m-a)!} p^{a+b} (1 - p)^{d-a-b} (1 - e)^{m+a-b} e^{d-m-a+b} \right] \\ &= \sum_{a=0}^{d-m} \sum_{b=0}^m \left[\binom{d}{m} \binom{m}{b} \binom{d-m}{a} p^{a+b} (1 - p)^{d-a-b} (1 - e)^{m+a-b} e^{d-m-a+b} \right] \\ &= \sum_{a=0}^{d-m} \sum_{b=0}^m \left[\binom{d}{m} \binom{m}{b} \binom{d-m}{a} (pe)^b ((1 - p)(1 - e))^{m-b} (p(1 - e))^a ((1 - p)e)^{d-m-a} \right] \\ &= \sum_{a=0}^{d-m} \sum_{b=0}^m \left[\binom{d}{m} \binom{m}{b} \binom{d-m}{a} (pe)^b ((1 - p)(1 - e))^{m-b} (p(1 - e))^a ((1 - p)e)^{d-m-a} \right] \\ &= \binom{d}{m} \left[\sum_{b=0}^m \binom{m}{b} (pe)^b ((1 - p)(1 - e))^{m-b} \right] \left[\sum_{a=0}^{d-m} \binom{d-m}{a} (p(1 - e))^a ((1 - p)e)^{d-m-a} \right] \\ &= \binom{d}{m} [pe + (1 - p)(1 - e)]^m [p(1 - e) + (1 - p)e]^{d-m} \end{aligned}$$

Therefore, we prove that $\Pr(Y^{\text{neighbor}} = m) = \binom{d}{m} [pe + (1 - p)(1 - e)]^m [p(1 - e) + (1 - p)e]^{d-m}$ which represents that $Y^{\text{neighbor}} \sim B(d, pe + (1 - p)(1 - e))$. Similarly, we can also prove that $Y^{\text{neighbor}} \sim B(d, p(1 - e) + (1 - p)e)$ when $Y_i = 1$. \square

Theorem 4. Given the true label $Y_i = 0$, the expectation of \hat{Y}_i can be calculated as $\mathbb{E}(\hat{Y}_i|Y_i = 0) = (1 - \alpha)e + \alpha[pe + (1 - p)(1 - e)]$. Similarly, when $Y_i = 1$, the expectation of \hat{Y}_i can be calculated as $\mathbb{E}(\hat{Y}_i|Y_i = 1) = (1 - \alpha)(1 - e) + \alpha[p(1 - e) + (1 - p)e]$. Furthermore, the variance of \hat{Y}_i can be represented as $\text{Var}(\hat{Y}_i) = (1 - \alpha)^2e(1 - e) + \frac{\alpha^2}{d}[pe + (1 - p)(1 - e)][p(1 - e) + (1 - p)e]$.

PROOF. When $Y_i = 0$, we have $\Pr(\tilde{Y}_i = 1|Y_i = 0) = e$ and $\Pr(\tilde{Y}_i = 0|Y_i = 0) = 1 - e$. Then the first part $\mathbb{E}[(1 - \alpha)\tilde{Y}_i|Y_i = 0] = (1 - \alpha)e$. Since we have proven that $Y^{\text{neighbor}} \sim B(d, pe + (1 - p)(1 - e))$, the second part $\mathbb{E}[\frac{\alpha}{d} \sum_{j \in [d]} \tilde{Y}_j|Y_i = 0] = \frac{\alpha}{d} \cdot d \cdot [pe + (1 - p)(1 - e)] = \alpha[pe + (1 - p)(1 - e)]$. By summing up these two parts, we obtain $\mathbb{E}(\hat{Y}_i|Y_i = 0) = (1 - \alpha)e + \alpha[pe + (1 - p)(1 - e)]$.

Similarly, when $Y_i = 1$, we have $\Pr(\tilde{Y}_i = 0|Y_i = 1) = e$ and $\Pr(\tilde{Y}_i = 1|Y_i = 1) = 1 - e$. Therefore, $\mathbb{E}[\tilde{Y}_i|Y_i = 1] = (1 - \alpha)(1 - e) + \frac{\alpha}{d} \cdot d \cdot [p(1 - e) + (1 - p)e] = (1 - \alpha)(1 - e) + \alpha \cdot [p(1 - e) + (1 - p)e]$.

The variance of \hat{Y}_i can be written as:

$$\begin{aligned} \text{Var}(\hat{Y}_i) &= (1 - \alpha)^2 \text{Var}(\tilde{Y}_i) + \frac{\alpha^2}{d^2} \text{Var}\left(\sum_{j \in [d]} \tilde{Y}_j\right) \\ &= (1 - \alpha)^2 e(1 - e) + \frac{\alpha^2}{d^2} \cdot d \cdot [pe + (1 - p)(1 - e)][p(1 - e) + (1 - p)e] \\ &= (1 - \alpha)^2 e(1 - e) + \frac{\alpha^2}{d} [pe + (1 - p)(1 - e)][p(1 - e) + (1 - p)e] \end{aligned}$$

□

Theorem. (Label Propagation and Denoising) Suppose the label noise is generated by T and the label propagation follows Equation 13. For a specific node i , we further assume the node has d neighbors, and its neighbor nodes have the probability p to have the same true label with node i , i.e., $\mathbb{P}[Y_i = Y_j] = p$. After one-round label propagation, the gap between the propagated label and the true label is expressed as

$$\mathbb{E}(Y - \hat{Y})^2 = \mathbb{P}(Y = 0)\mathbb{E}(\hat{Y}|Y = 0)^2 + \mathbb{P}(Y = 1)\left(\mathbb{E}(\hat{Y}|Y = 1) - 1\right)^2 + \text{Var}(\hat{Y}), \quad (16)$$

where

$$\mathbb{E}(\hat{Y}_i|Y_i = 0) = (1 - \alpha)e + \alpha[pe + (1 - p)(1 - e)], \quad (17a)$$

$$\mathbb{E}(\hat{Y}_i|Y_i = 1) = (1 - \alpha)(1 - e) + \alpha[p(1 - e) + (1 - p)e], \quad (17b)$$

$$\text{Var}(\hat{Y}_i) = (1 - \alpha)^2 e(1 - e) + \frac{\alpha^2}{d} [pe + (1 - p)(1 - e)][1 - pe - (1 - p)(1 - e)]. \quad (17c)$$

PROOF.

$$\begin{aligned} \mathbb{E}(\hat{Y} - Y)^2 &= \mathbb{P}(Y = 0)\mathbb{E}\left((\hat{Y} - Y)^2|Y = 0\right) + \mathbb{P}(Y = 1)\mathbb{E}\left((\hat{Y} - Y)^2|Y = 1\right) \\ &= \mathbb{P}(Y = 0)\mathbb{E}\left(\hat{Y}^2|Y = 0\right) + \mathbb{P}(Y = 1)\mathbb{E}\left((\hat{Y} - 1)^2|Y = 1\right) \\ &= \mathbb{P}(Y = 0)\left[\mathbb{E}(\hat{Y}|Y = 0)^2 + \text{Var}(\hat{Y}|Y = 0)\right] + \mathbb{P}(Y = 1)\left[\mathbb{E}(\hat{Y} - 1|Y = 1)^2 + \text{Var}(\hat{Y}|Y = 1)\right] \\ &= \mathbb{P}(Y = 0)\mathbb{E}(\hat{Y}|Y = 0)^2 + \mathbb{P}(Y = 1)\left(\mathbb{E}(\hat{Y}|Y = 1) - 1\right)^2 + \text{Var}(\hat{Y}), \end{aligned}$$

The detailed expectation and variance of \hat{Y}_i have been proved in the above. □

E.2 Proof of Theorem 2

Theorem. (Generalization Error and Oracle Inequality) Denote the node feature X sampled from the distribution D , the graph topology as A , the set of training nodes as S_n , the neural network as $f(\cdot, \cdot)$, and $\hat{f} = \inf_f \sum_{X \in S_n} (\hat{Y} - f(X, A))$. Assume that the propagated label concentrated on its mean, i.e., with probability at least $\frac{\delta}{2}$, $\|\hat{Y} - Y\| - \mathbb{E}|\hat{Y} - Y| \leq \epsilon_1$. We further assume the generalization error is bounded with respect to the propagated labels, i.e., with probability at least $\frac{\delta}{2}$,

$$\mathbb{E}_{X \sim D} |\hat{Y} - \hat{f}(X, A)| - \inf_f \mathbb{E}_{X \sim D} |\hat{Y} - f(X, A)| \leq \epsilon_2. \quad (18)$$

Then we obtain the generalization error bound for training with noisy labels and test on the clean labels, i.e., with probability at least δ , the generalization error trained with propagated labels is given by

$$\mathbb{E}_{X \sim D} |Y - \hat{f}(X, A)| \leq \inf_f \mathbb{E}_{X \sim D} |Y - f(X, A)| + \epsilon_2 + 2(\mathbb{E}|\hat{Y} - Y| + \epsilon_1). \quad (19)$$

PROOF. We denote $f^* = \inf_f \mathbb{E}_{X \sim D}(Y - f(X, A))$, $f' = \inf_f \mathbb{E}_{X \sim D}(\hat{Y} - f(X, A))$. Then

$$\mathbb{E}_{X \sim D}|Y - \hat{f}(X, A)| \leq \mathbb{E}_{X \sim D}|\hat{Y} - \hat{f}(X, A)| + |Y - \hat{Y}| \quad (20)$$

$$\stackrel{(a)}{\leq} \mathbb{E}_{X \sim D}|\hat{Y} - f'(X, A)| + \epsilon_2 + |Y - \hat{Y}| \quad (21)$$

$$\stackrel{(b)}{\leq} \mathbb{E}_{X \sim D}|\hat{Y} - f^*(X, A)| + \epsilon_2 + |Y - \hat{Y}| \quad (22)$$

$$\leq \mathbb{E}_{X \sim D}|Y - f^*(X, A)| + |Y - \hat{Y}| + \epsilon_2 + |Y - \hat{Y}| \quad (23)$$

$$= \mathbb{E}_{X \sim D}|Y - f^*(X, A)| + \epsilon_2 + 2|Y - \hat{Y}| \quad (24)$$

$$\stackrel{(c)}{\leq} \mathbb{E}_{X \sim D}|Y - f^*(X, A)| + \epsilon_2 + 2(\mathbb{E}|Y - \hat{Y}| + \epsilon_1) \quad (25)$$

where (a) follows the generalization bound with respect to propagated labels, (b) follows $\inf_f \mathbb{E}_{X \sim D}|\hat{Y} - f(X, A)| \leq \mathbb{E}_{X \sim D}|\hat{Y} - f^*(X, A)|$, and (c) follows the concentration of $|Y - \hat{Y}|$. The probability δ is obtained by union bound. \square